Available online at www.sciencedirect.com
ScienceDirect
Journal of Nuclear Materials 372 (2008) 256–262
journal of nuclear materials
www.elsevier.com/locate/jnucmat

Microstructure of long-term annealed highly irradiated beryllium

A. Leenaers *, G. Verpoucke, A. Pellettieri, L. Sannen, S. Van den Berghe

SCK·CEN, Reactor Materials Research, Boeretang 200, B-2400 Mol, Belgium

Received 6 December 2006; accepted 20 March 2007

Abstract

The Material Testing Reactor BR2 of SCK·CEN has a beryllium matrix which has been replaced in 1995. Pieces of this matrix, which were irradiated over a period of 15 yr at about ±50 °C up to a fast neutron fluence ($E > 1$ MeV) of 4.67×10^{22} n/cm^2, have been retrieved for creep and microstructure studies. An amount of helium resulting from transmutation has accumulated up to approximately 2.2 at.% which is comparable to the expected He content of a fusion reactor blanket at its end of life. Post-irradiation anneals have been performed at 500, 750 and 900 °C, with an annealing time ranging between 50 hours and three months. Microstructural analyses show a clear evolution in bubble growth and He diffusion towards the grain boundaries where the bubbles coalesce. Complete release of ^{4}He is observed at temperatures >750 °C, resulting in a stagnation of the beryllium swelling. The microstructural changes are mainly temperature driven. Only at high annealing temperature, an influence of the annealing time is observed.

1. Introduction

Due to its excellent neutron thermalisation, multiplication properties and good thermal characteristics, beryllium is considered as a plasma facing material and as a neutron multiplier in the design of future thermonuclear fusion reactors. The most important irradiation induced effects on beryllium are associated with the high quantity of helium produced through the neutron multiplication reaction ^{9}Be(n,2n)2^{4}He and the reaction chain ^{9}Be(n,α)^{6}He(β$^-$)^{6}Li(n,α)^{3}H. The solubility of helium in beryllium is very limited and supersaturation of the Be matrix is attained very quickly. The helium atoms generated are allowed to diffuse and precipitate in bubbles, grow and coalesce and as such induce swelling of the material. Usually, swelling in neutron-irradiated materials is interpreted in terms of two general mechanisms. The first is a direct consequence of the configurational entropy brought about by radiation damage [1,2]. High energy neutrons knock out atoms in the beryllium crystal lattice, generating defects such as vacancies. Through the classical nucleation mechanism of vacancy accumulation, voids are formed. The second type of swelling is a consequence of the gaseous nuclear reaction products that are formed [1]. Gas production plays a more important role than radiation damage in limiting the lifetime of the component. Several studies have already been conducted to evaluate the influence of helium production on the microstructure of beryllium under irradiation in both operating and accidental conditions, but open literature data on highly irradiated beryllium in the temperature range of interest, are scarce. In this article, an assessment of the dimensional stability and microstructure properties of both annealed and non-annealed irradiated beryllium has been made by means of helium content measurements, density measurements and microstructural characterisation.

2. Experimental

2.1. The samples

The beryllium samples used in this work were part of the second matrix (1980–1995) of the Materials Testing Reactor (MTR) BR2 at SCK·CEN. The original material is a

* Corresponding author. Tel.: +32 14 333044; fax: +32 14 321216.
E-mail address: aleenaer@sckcen.be (A. Leenaers).

0022-3115/$ - see front matter © 2007 Elsevier B.V. All rights reserved.
doi:10.1016/j.jnucmat.2007.03.214

Table 1
Chemical composition in wt% of S-200-E grade beryllium as supplied by the manufacturer American Beryllium Company Inc.

Be	BeO	Fe	C	Al	Mg	Si	Other metallic elements
> 98	< 2.0	< 0.18	< 0.15	< 0.15	< 0.08	< 0.08	< 0.04 Each

S-200-E grade Be (chemical composition see Table 1), manufactured by vacuum hot-pressing of impact attritioned Be powder of at least 100 mesh. The average grain size amounts to 10–13 μm. During the nearly 15 years in the reactor, the beryllium matrix has been subjected to a temperature of approximately 50 °C and to a fission neutron fluence of 5.32×10^{22} n/cm^2. This value was converted into fast neutron fluence by multiplying it by 0.878, a value based on the calculated average BR2 spectrum, resulting in a fast fluence ($E > 1$ MeV) of 4.67×10^{22} n/cm^2 [3]. As the irradiation of the Be samples has taken place at low temperatures (≈50 °C), post-irradiation annealing steps are required to use the BR2 matrix beryllium as representative material for the fusion reactor operating and accidental conditions.

It should be noted at this point that the swelling expected in the Be matrix should not only be attributed to the production of ^{4}He atoms but also to ^{3}H production. The material under investigation has accumulated a helium content which can be compared to the amount produced in a fusion blanket at its end-of-life, but was generated over a much longer irradiation time and at lower temperature as well as by a different neutron spectrum. Part of this discrepancy is resolved by the anneals, but a further consequence of the fission-irradiated Be is that a much higher ^{3}H production is expected, compared to what would be generated in a fusion reactor during the period required for the production of a similar He content [4]. It was therefore decided to focus only on the behaviour of He in this study.

2.2. Annealing

The irradiated beryllium samples were annealed in a horizontal tubular furnace (Adamel type M05HT) at 500, 750 and 900 °C for periods ranging between 50 h and three months (Table 2). The quartz tube interior was pumped down to a vacuum of approximately 6×10^{-6} mbar. To protect the seal and as such to maintain the vacuum, the head of the tube is water cooled. The annealing program started with a positive ramp of 20 °C/h up to the selected annealing temperature (t_{anneal}). During the dwell time, the temperature inside the sample chamber was kept constant to $t_{anneal} \pm 5$ °C. At the end of the program, a ramp down of 20 °C/h was executed.

Table 2
Annealing data of the irradiated Be samples

Dwell time (h)	Annealing temperature		
	500 °C	750 °C	900 °C
50	x	x	x
200	x	x	x
720			x
2106	x		x

2.3. Retained helium content

The retained ^{4}He content in the annealed and as-received beryllium specimens was measured by hot vacuum extraction according to ASTM E146. From literature [5] it can be found that for a complete release of all retained gas within a reasonable time, a temperature just below the beryllium melting point (1278 ± 5 °C) is required. Along with the fact that release of the trapped He will occur at the hcp–bcc transformation temperature (1268 °C) [6], it was decided to perform the measurements at 1275 °C. The released gas is transferred by a Hg-diffusion pump into a calibrated volume. By measuring the pressure of this volume, the total amount of released gas was determined. The fraction of helium in this total volume was measured by quadrupole mass-spectrometry. The method was calibrated using certified unalloyed titanium standards (NBS352-353-354) resulting in a relative accuracy (1σ) of the helium measurements of ±4%.

The measured retained ^{4}He content in the irradiated Be prior and after annealing are summarized in Table 3.

2.4. Density measurement

The densities of the irradiated and annealed beryllium samples were measured by means of a mercury pycnometer installed in a hot cell [5]. This pycnometer is a device inside which a plunger (i.e. an accurately uniformly dimensioned metallic bar) is driven mechanically into a mercury containing plunger channel, displacing the mercury into an evacuated and sealed specimen chamber until it is completely filled up. The sample volume is obtained from the product of the plunger cross-sectional area and the difference in plunger displacement with and without the sample present in the chamber. The pycnometer is calibrated using stainless steel standards. The relative accuracy of the measurements amounts to ±0.2% (1σ). Prior to the analysis, the samples have been accurately weighted. From the measured sample volume and weight, the density of the specimen is calculated (Table 3).

A theoretical density of 1.862 g/cm^3 can be calculated based on the content of the samples (Table 1) of 98% beryllium metal ($\rho = 1.8477$ g/cm^3) and 2% beryllium oxide ($\rho = 3.009$ g/cm^3). The measured density of 1.852 g/cm^3

Table 3
Results of helium and density measurements and calculated swelling with respect to the density of the as-fabricated material (1.852 g/cm^3)

Annealing		Retained ^{4}He (at.%) ($\pm1\sigma$)	Density (g/cm^3) ($\pm1\sigma$)	Swelling (%)	
t (h)	T (°C)			Measured	Calculated
15 yr	50	2.2479 ± 0.1047	1.818 ± 0.002	1.7 ± 0.1	2.7
50	500	2.1647 ± 0.0649	1.759 ± 0.001	5.0 ± 0.1	7.6
200	500	2.4473 ± 0.0734	1.743 ± 0.002	6.0 ± 0.1	7.6
50	750	1.4844 ± 0.0445	1.360 ± 0.001	26.6 ± 0.1	27.6
200	750	1.4836 ± 0.0445	1.351 ± 0.001	27.1 ± 0.1	27.6
50	900	1.0810 ± 0.0324	1.339 ± 0.001	27.6 ± 0.1	54.3
200	900	0.0016 ± 0.0001	1.323 ± 0.002	28.7 ± 0.1	54.3
2106	900	0.0036 ± 0.0003	1.296 ± 0.006	30.3 ± 0.6	54.3

[5,3] of the as-fabricated material thus corresponds to 99.5% of the theoretical density.

2.5. Image analysis

The microstructure of the samples was evaluated by means of optical microscopy, and scanning electron microscopy combined with image analysis. Sample preparation comprised embedding of the beryllium specimen in a conductive resin using hot-pressing. The samples were then polished with SiC paper of successively finer grain size, finishing on cloth with diamond paste of consecutively 3 μm and 1 μm particle size.

Optical microscopy was performed on a Reichert Telatom 3 remote-controlled and shielded optical microscope. For scanning electron microscopy (SEM), a shielded JEOL 6310 scanning electron microscope was used. Because of their great depth of focus, high contrast and homogeneous brightness, the secondary electron (SE) images were used for further image analysis. The magnification of the SE images was chosen in such a way that a sufficiently large number of bubbles was visible in the image to produce statistically justified results by the image analysis (SigmaScan Pro software package). The SEM images were converted to binary images on which binary filters were applied. From the latter image, the area occupied by pores as well as their Feret diameter (i.e. the theoretical diameter of the object if it would be circular in shape, $\mathrm{FD} = \sqrt{\frac{4\times \mathrm{Area}_{\mathrm{measured}}}{\pi}}$), were measured.

In a metallurgical system, when a sample is sectioned, not all particles/grains are sectioned through their maximum diameter, causing many to appear smaller than they actually are. Any experimental measurement of size or size distribution will, therefore, be skewed to smaller sizes. The measured distribution of sizes can be corrected using the Schwartz–Saltykov method. The Saltykov area analysis is a classical method to construct a 3D inclusion volumetric distribution from a 2D area distribution [7]. It is applicable, not only to spherical inclusions but also, in principle, to convex ones in polydispersed systems. From the corrected size distribution data, the mean diameter of the bubbles/pores in the annealed beryllium samples was calculated.

3. Results

Beryllium subjected to a temperature of ≈50 °C and to neutron fluences higher than 10^{22} n/cm^2 ($E > 0.1$ MeV), exhibits no significant swelling (Table 3) but undergoes considerable hardening (Fig. 1) and embrittlement. The produced He atoms are trapped at vacancies within the Be lattice causing high internal stresses and hardening [8,9]. The measured hardness value of the sample annealed at 750 °C is consistent with the hardness of the non-irradiated specimen, which underwent a heat treatment at ≈750 °C during its production [10].

During thermal annealing, the He atoms trapped in the beryllium lattice or on dislocations become mobile and diffuse to the grain boundaries or/and precipitate into bubbles. The bubbles observed at the grain boundaries are created by migration of He atoms to voids and/or interfaces of particles such as BeO present at the grain boundaries [11]. These gas bubbles, which coarsen and coalesce, induce a swelling of the material.

The retained ^{4}He measurements (Fig. 2) show that at least part of the helium is released at an annealing temperature higher than 500 °C. No more retained He is observed after the heat treatment of 200 h at 900 °C. The neutron

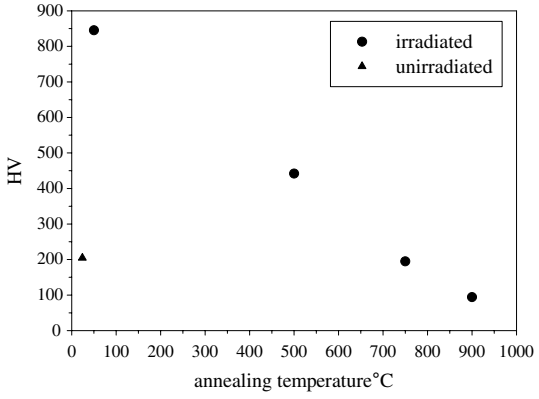

Fig. 1. Measured Vickers hardness of beryllium as function of annealing temperature. The applied load was 50 gF for the samples annealed at 900 °C, for all other samples a load of 200 gF was applied.

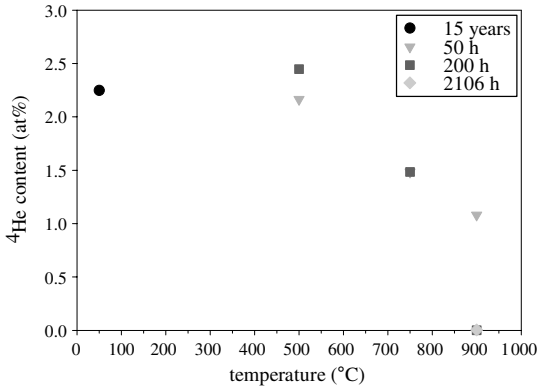

Fig. 2. Measured ^{4}He content after annealing of the Be specimen (see also Table 3).

fluence required to build up the measured ^{4}He content C of about 2.2 at.% can be calculated using [3]:

$$C\ [\text{at.}\%] = (0.4880 \pm 0.0090) \times \Phi \times 10^{-22} \quad (1)$$

with Φ in n/cm^2 ($E > 1$ MeV). This results in a calculated fast neutron fluence of 4.6×10^{22} n/cm^2, which is in good agreement with the result calculated on the basis of reactor physics yielding 4.67×10^{22} n/cm^2.

The swelling caused by annealing is calculated (Table 3) from the measured density (ρ_m) value and the density of the as-fabricated material ($\rho = 1.852$ g/cm^3) using $S = \frac{\rho - \rho_m}{\rho} \times 100$. It is noticed that the swelling of the material progresses slowly for annealing temperatures below 500 °C (Fig. 3(a)). Above 500 °C, a steep increase occurs, but for temperatures above 750 °C the measured swelling (or density) shows a saturation. At this point, the release of the complete He content prevents further swelling of the beryllium.

The observed swelling of the specimens can be compared to a theoretical value which is obtained using the empirical relation [3]:

$$S_{\text{theoretical}} = (0.58 \pm 0.03) \times \Phi \times 10^{-22} + (0.372 \pm 0.005) \times 10^{-55} \times \Phi^2 \times t^4 \quad (2)$$

with σ the fast neutron fluence calculated from helium content measurements (4.6×10^{22} n/cm^2) and t the annealing temperature in °C. The observed swelling below 750 °C is in good agreement with the calculated values (see Table 3, Fig. 3(a)). Since the swelling is essentially temperature driven, there is no time dependence in the equation.

From the optical microscopy images of the as-irradiated samples (Fig. 4(a)), it was clearly observed that bubble formation at the grain boundaries has occurred as a result of irradiation. However, at the low irradiation temperatures (≈50 °C), He atoms are most probably trapped at immobile vacancies within the Be lattice and as such cannot contribute to the gas bubble formation at the grain boundaries [12]. It is suggested that hydrogen, which is quite mobile at these low temperatures, may be the gas involved in the grain boundary bubbles of the irradiated Be [8]. The density measurement of the irradiated Be prior to annealing shows a swelling of 1.9%.

Annealing of the material at a temperature of 500 °C did not result in visible changes of the microstructure of the specimen (Fig. 4(b)). At an annealing temperature of 750 °C (Fig. 4(c)), the bubbles sizes at the boundaries have visibly increased and intragranular bubbles have formed. By scratching the polished surface and as such exposing the grain surface, it was found that the intragranular bubbles have a hexagonal shape which results from the crystal structure (hcp) of beryllium.

At 900 °C (Fig. 4(d)), the bubble growth observed at the grain boundaries is most probably due to coalescence of the smaller bubbles as well as additional He diffusion. As the shape of these larger pores is no longer spherical but more lenticular, one can assume that they are part of a network of interconnected grain boundary bubbles and, at 900 °C, escape paths for the He gas are created. This

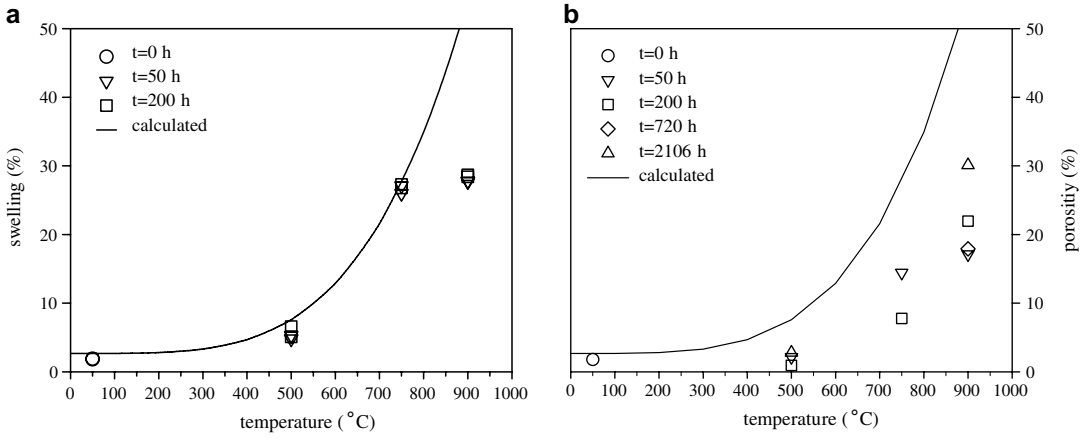

Fig. 3. Swelling values obtained from density measurements (a) and porosity based on image analysis (b) of beryllium samples annealed at different temperatures and times. The solid line is the theoretical swelling calculated using Eq. (2).

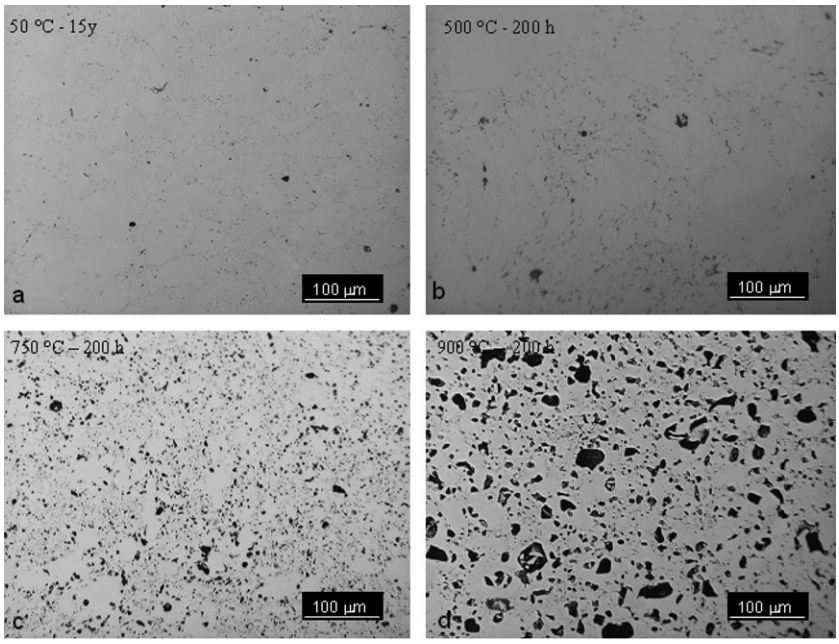

Fig. 4. Optical image of the samples annealed for 200 h at 500 °C (b), 750 °C (c) and 900 °C (d). As a reference the image of the as-received material is given (a).

assumption is confirmed by the observed saturation of the swelling after annealing at 900 °C (Fig. 3(a)) and the full release of the retained ^{4}He (Fig. 2).

The SEM images (Fig. 5) reveal the same evolution in bubble growth with increasing annealing temperature as observed by optical microscopy. However, due to the sensitivity of the technique in terms of density contrast, the images also show BeO particles located at the grain boundaries, which is typical for powder metallurgy produced beryllium. Furthermore, it should be noted that the BeO particles appear to coalesce, forming larger precipitates on the grain boundaries with increasing annealing temperatures.

The annealing time has no visible influence on the microstructure of the annealed Be, nor on the swelling behaviour of the material. This supports the notion that at high temperature, swelling is a rapid process, which is completed in the first hours of the anneal.

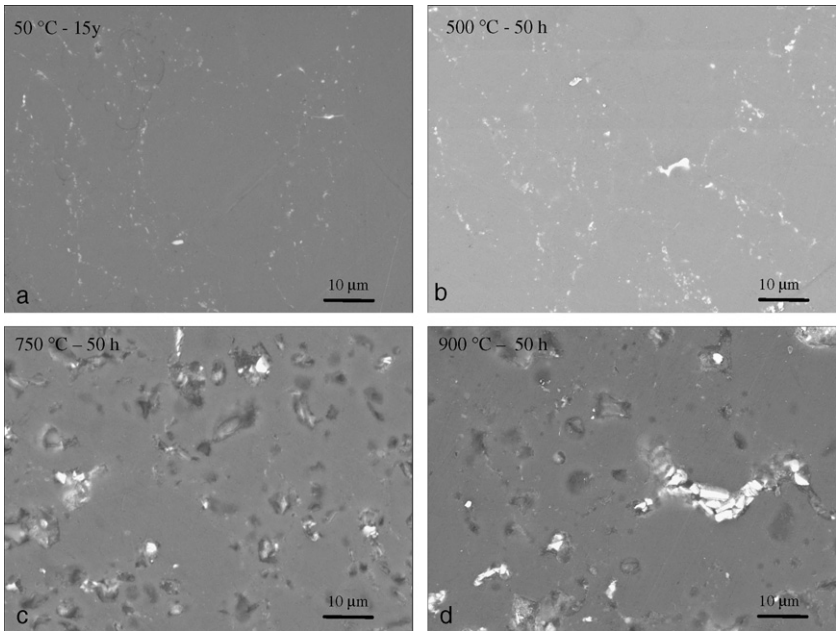

Fig. 5. Secondary electron images of irradiated beryllium as-received (a) and annealed at 500 °C (b), 750 °C (c) and 900 °C (d) for 50 h.

4. Discussion

The Schwartz–Saltykov diameter analysis is performed on the SEM images to obtain a statistical mean diameter of the observed gas bubbles and pores. In Fig. 6(a), it is observed that the mean diameter increases with temperature. The annealing time shows no influence on the mean pore diameter (Fig. 6(b)).

The volumetric distribution of the different pore diameters (Feret diameters) shows that at an annealing temperature of 500 °C (Fig. 7(a)), the majority of the gas atoms is located in bubbles with a Feret diameter smaller than 5 μm. At 750 °C, the largest Feret diameter found is approximately 20 μm with a maximum in the distribution at ±5 μm (Fig. 7(b)) while the largest Feret diameter measured has increased to approximately 50 μm at 900 °C (Fig. 7(c)). However, the maximum of the distribution at 900 °C seems to depend on the annealing time; this is between 10 and 15 μm at 50 h (Fig. 7(c)), 200 h (Fig. 7(d)) and 720 h (Fig. 7(e)), but the distribution curves for the samples annealed at 200 h and 720 h start to show a more important tail towards larger pore sizes. This tail, centered around 20 and 25 μm, respectively, becomes most clear in the distribution graph of the 900 °C annealing at 2160 h (Fig. 7(f)).

Also, a value for the porosity of the samples was calculated from the image analysis. Fig. 3(b) shows the increase of the observed porosity with annealing temperature. At 900 °C, the porosity volume fraction increases with the annealing time.

The obtained porosity volume fraction values can be directly compared to the swelling calculated from the density measurements (Fig. 3(a)). It is noticed for annealing temperatures below 900 °C that, all values from image analysis are systematically lower than the numbers resulting from the density measurement. This shows that not all of the helium bubbles can be detected by image analysis. At annealing temperatures below 900 °C, a large amount of the gas atoms has migrated into nanometer size bubbles, which are too small to be detected by scanning electron microscopy. Transmission electron microscopy will be performed on some of the samples of this study [13].

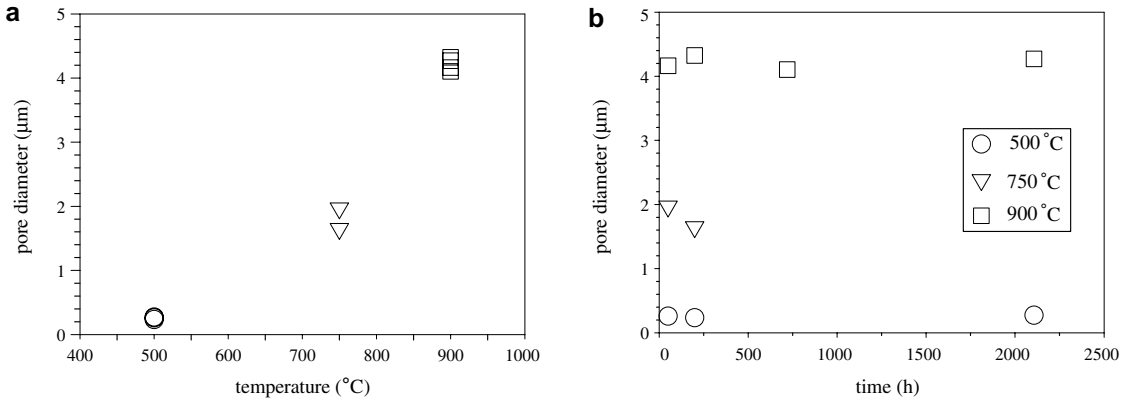

Fig. 6. Statistical mean diameter of the pores observed in the annealed samples as function of temperature (a) and annealing time (b).

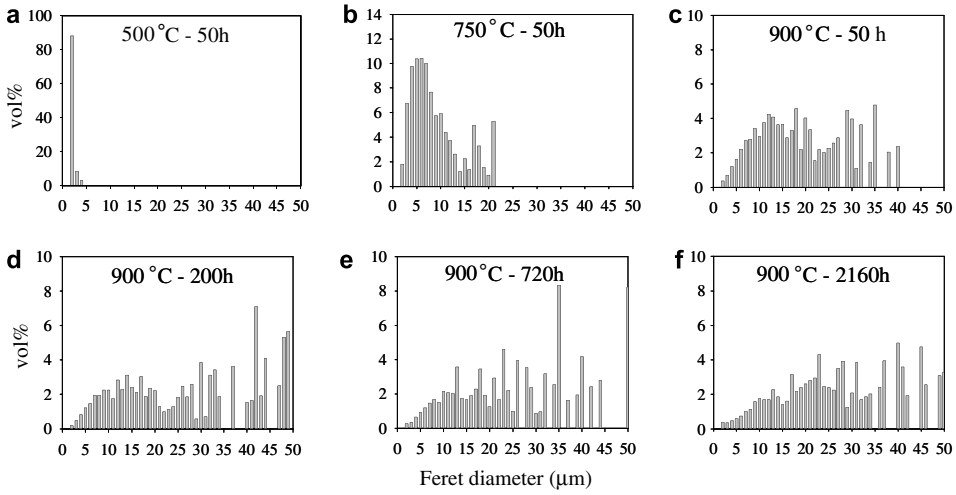

Fig. 7. Volumetric distribution of the pores according to their Feret diameter, for samples annealed at 500 °C (a), 750 °C (b) and 900 °C (c) for 50 h and annealed at 900 °C for 200 h (d), 720 h (e) and three months (f).

The swelling values resulting from image analysis do not show the saturation at 900 °C (Fig. 3(b)). The porosity measured for the sample annealed for three months indicates that there is still swelling of the material relative to the samples annealed at 750 °C. This appears to be in contradiction with the full release of the retained ^{4}He measured. A possible explanation for the observed increase in swelling could be that during the long-term anneal at high temperatures (>2/3 of the melting temperature in K) sintering occurs, causing the nanometer-sized voids to migrate to either the grain boundary where they coalesce with the intergranular bubbles or to the existing large intragranular bubbles. This assumption is consistent with the observation of the larger pore sizes (the tail in the Feret diameter distribution) found in this sample. Furthermore, when comparing the measured swelling $(1-\frac{\rho_m}{\rho})$ based on the density measurements with the absolute value of the porosity (P) as determined by image analysis, a good correlation $\frac{\rho_m}{\rho}=(1-P)$ between the values is found.

5. Conclusion

Samples of the refurbished beryllium matrix of the BR2 reactor at SCK·CEN, irradiated over a period of 15 years at about ≈50 °C up to a fast neutron fluence ($E>1$ MeV) of 4.67×10^{22} n/cm^2, have been annealed and submitted to microstructure analysis.

Annealing of the samples at 500 °C causes the ^{4}He atoms to migrate to the grain boundaries and precipitate into small bubbles. The observed intergranular bubbles are larger at 750 °C and start to coalesce, and intragranular bubbles are formed.

At an annealing temperature of 900 °C even larger bubbles are formed at the grain boundaries by coalescence and they start to interlink. The intragranular bubbles do not migrate to the grain boundaries but merge and form isolated large intragranular bubble. Retained ^{4}He measurements show that the latter samples have experienced a complete release of ^{4}He during the anneal, and a saturation of the swelling was calculated from the density measurements.

The changes observed in the microstructure of the annealed beryllium samples, are mainly influenced by the annealing temperature. Some influence of the annealing time is noticeable only at high annealing temperature (900 °C). Image analysis on the microscopy images of the sample annealed at 900 °C for 2160 h shows that there is still a microstructural evolution in the material. This could be explained by assuming that sintering causes nanometer-sized voids to migrate to either the grain boundary where they coalesce with the intergranular bubbles or to the existing large intragranular bubbles, resulting in the observed increase of the visible porosity without density changes.

References

[1] F. Scaffidi-Argentina, M. Dalle Donne, C. Ferrero, C. Ronchi, Fus. Eng. Des. 27 (1995) 275.
[2] R. Kemp, G. Cottrell, K.D.H. Bhadeshia, Energ. Mater. 1 (2) (2006) 103.
[3] L. Sannen, C. De Raedt, F. Moons, Y. Yao, Fus. Eng. Des. 29 (1995) 470.
[4] E. Rabaglino, Forschungszentrum Karlsruhe, Report FZKA 6939, 2004.
[5] L. Sannen, C. De Raedt, in: M. Gasparotto, H. Knoepfel (Eds.), Proceedings of the 17th Symposium on Fusion Technology, Roma, Italy, 1992, p. 1474.
[6] H. Kleykamp, J. Nucl. Mater. 294 (2001) 88.
[7] E. Underwood, in: M. Cohen (Ed.), Quantitative Stereology, Addison-Wesley Publishing Company, Massachusetts, 1970.
[8] J.B. Mitchel, J. Fus. Energ. 5 (4) (1986) 327.
[9] D.V. Andreev, V.N. Bespalov, A.J. Birjukov, B.A. Gurovich, P.A. Platonov, J. Nucl. Mater. 233–237 (1996) 880.
[10] D.D. Lemon, W.F.J. Brown, J. Test. Eval. 13 (2) (1985) 152.
[11] W. Kesternich, H. Ullmaier, J. Nucl. Mater. 312 (2003) 212.
[12] V.P. Chakin, Z.Y. Ostrovsky, J. Nucl. Mater. 307–311 (2002) 657.
[13] W. Van Renterghem, A. Leenaers, S. Van den Berghe, J. Nucl. Mater., submitted for publication.